

Optical study of the charge-density-wave mechanism in $2H\text{-TaS}_2$ and Na_xTaS_2

W. Z. Hu,¹ G. Li,¹ J. Yan,¹ H. H. Wen,¹ G. Wu,² X. H. Chen,² and N. L. Wang^{1,*}

¹*Beijing National Laboratory for Condensed Matter Physics, Institute of Physics, Chinese Academy of Sciences, Beijing 100080, People's Republic of China*

²*Hefei National Laboratory for Physical Science at Microscale and Department of Physics, University of Science and Technology of China, Hefei 230026, People's Republic of China*

(Received 6 February 2007; revised manuscript received 1 May 2007; published 13 July 2007)

We report an optical study of transition metal dichalcogenide $2H\text{-TaS}_2$ and the Na intercalated superconductor Na_xTaS_2 over a broad frequency range at various temperatures. A clear gap feature was observed for $2H\text{-TaS}_2$ when it undergoes the charge-density wave (CDW) transition. The existence of a Drude component in $\sigma_1(\omega)$ below T_{CDW} indicates that the Fermi surface of $2H\text{-TaS}_2$ is only partially gapped in the CDW state. The spectral evolution of two different Na_xTaS_2 crystals further confirms that the partial gap structure observed in $2H\text{-TaS}_2$ has a CDW origin. The CDW mechanism for $2H\text{-TaS}_2$ and the competition between CDW and superconductivity in the Na_xTaS_2 system are discussed.

DOI: [10.1103/PhysRevB.76.045103](https://doi.org/10.1103/PhysRevB.76.045103)

PACS number(s): 78.30.Er, 71.45.Lr, 74.25.Gz, 78.40.Kc

I. INTRODUCTION

Charge-density-wave (CDW) order and its coexistence with superconductivity in $2H$ -type transition metal dichalcogenides (TMDCs) has been one of the major subjects in condensed matter physics since the 1970s. The name $2H$ is derived from the structural character, where 2 represents two chalcogen-metal-chalcogen sandwiches in one unit cell and H stands for "hexagonal." Among the CDW-bearing members in this family, $2H\text{-TaSe}_2$ has an incommensurate followed by a commensurate CDW transition at 122 and 90 K, respectively, while $2H\text{-TaS}_2$ and $2H\text{-NbSe}_2$ only undergo one incommensurate CDW transition at 75 and 33 K, respectively,¹ on the contrary, the superconducting transition temperature T_c increases from $2H\text{-TaSe}_2$ through $2H\text{-TaS}_2$ to $2H\text{-NbSe}_2$, suggesting that the CDW order and superconductivity compete. Additionally, upon intercalation of Na into $2H\text{-TaS}_2$, T_{CDW} is suppressed but T_c increases from 0.8 to 4.4 K, yielding further evidence for the competition between these two orders.² Although it is generally believed that the superconductivity in $2H\text{-TMDC}$ is caused by the conventional electron-phonon coupling, the driving mechanism for the CDW transition is still not well understood. Different viewpoints including the Fermi surface (FS) nesting,³ the saddle point mechanism,⁴ or other hidden orders in the k space^{5,6} have been proposed to explain the CDW instability, but no consensus has been reached.

Optical spectroscopy is a powerful bulk sensitive technique with high energy resolution. It is widely used to probe the carrier dynamics and possible gap formation of an electronic system. Previous studies on the in-plane optical responses of $2H\text{-NbSe}_2$ (Ref. 7) and $2H\text{-TaSe}_2$ (Ref. 8) did not reveal any sharp changes associated with the CDW transitions. As $2H\text{-TaS}_2$ has only one CDW transition with a relatively higher T_{CDW} , it is therefore an ideal system to study the CDW mechanism in $2H\text{-TMDC}$ family. However, no detailed optical research was performed on $2H\text{-TaS}_2$, except some early work on the high energy structure at room or liquid N_2 temperatures.⁹ In this work, we report a detailed optical study of $2H\text{-TaS}_2$ and Na_xTaS_2 over a broad fre-

quency range at various temperatures to reveal the CDW mechanism. The overall frequency dependent reflectivity $R(\omega)$ of $2H\text{-TaS}_2$ shows a metallic response, but a suppression in the midinfrared emerges below T_{CDW} . The real part of conductivity $\sigma_1(\omega)$ is composed of a Drude response together with a midinfrared peak in the CDW state, indicating the formation of a partial gap on the Fermi surface. For Na_xTaS_2 , the CDW features turn weaker and tend to disappear as Na content increases. All those optical results, being consistent with the transport measurements obtained on the same crystals, can be well understood in the frame of FS nesting mechanism.

II. EXPERIMENT AND RESULTS

$2H\text{-TaS}_2$ single crystals were grown by the chemical iodine-vapor transport method. High purity Ta (99.95%) and S (99.5%) powders were mixed, thoroughly ground, pressed into a pellet, and sealed under vacuum in a quartz tube ($\varnothing 13 \times 150 \text{ mm}^2$) with iodine (10 mg/cm^{-3}). Single crystals were obtained after growing at 720–700 °C for a week and slowly cooling down to room temperature at a rate of 1 °C/h. $2H$ type Na_xTaS_2 single crystals were grown by the chemical reaction method, as described previously.² The T -dependent resistivity was obtained by the four contacts technique in a Quantum Design PPMS, and the results are shown in Fig. 1. There is a clear CDW transition at 75 K for $2H\text{-TaS}_2$, while such feature is vague around 65 K for Na_xTaS_2 $T_c=2$ K sample, and totally disappears in the higher Na content crystals ($T_c=4.2$ K). The superconducting transition temperature for Na_xTaS_2 was identified by the ac susceptibility as shown in the inset of Fig. 1.

The near-normal incident reflectance spectra were measured on as-grown surfaces using a Bruker 66v/s spectrometer in the frequency range from 30 to 25 000 cm^{-1} . An *in situ* gold and aluminum overcoating technique was used for the experiment. Considering the small size of our samples (about $1.5 \times 2 \text{ mm}^2$), the data below 150 cm^{-1} are cut off for reliability. The T -dependent $R(\omega)$ for $2H\text{-TaS}_2$ and Na_xTaS_2 are shown in Fig. 2. They are all metallic in

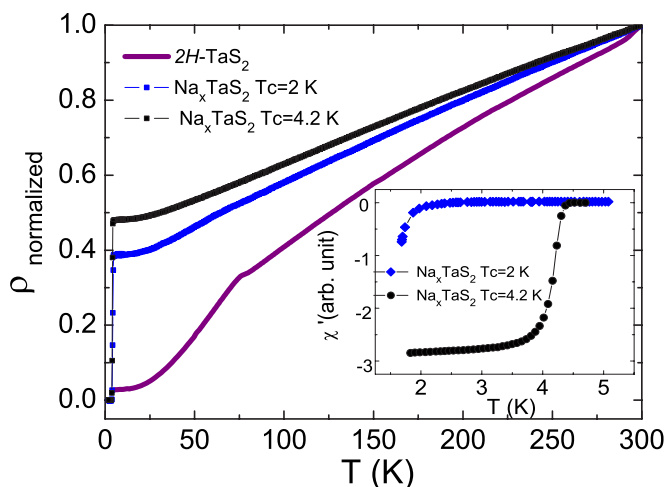


FIG. 1. (Color online) T -dependent resistivity for $2H$ - TaS_2 and two Na_xTaS_2 crystals (all normalized to respective values at 300 K). The inset shows the real part of ac susceptibility below 5 K, which identifies T_c for two Na_xTaS_2 crystals as 2 and 4.2 K, respectively.

nature, with high reflectivity at low frequencies and well-defined reflectance edges (plasma edge) in the near-infrared region. The difference between the pure and intercalated materials in low energies is evident. For $2H$ - TaS_2 , $R(\omega)$ at 10 and 60 K are suppressed below that of 90 K from 400 to 5000 cm^{-1} . This is a typical FS partial-gap behavior manifested in reflectance.¹⁰ Similar suppression is weak in Na_xTaS_2 $T_c=2$ K sample, and almost invisible in $T_c=4.2$ K sample with higher Na content.

Figure 3 illustrates the real part of conductivity obtained by the Kramers-Kronig transformation of $R(\omega)$ at selected temperatures. The insets show $\sigma_1(\omega)$ below 4000 cm^{-1} at 10 K. A Drude contribution exists at all temperatures for both $2H$ - TaS_2 and Na_xTaS_2 , thus confirming their metallic behavior. For $2H$ - TaS_2 , a midinfrared peak emerges below T_{CDW} and vanishes at higher T . In order to clarify this feature, we use a Drude model to fit the low frequency part of the 10 K curve, and subtract this free-carrier contribution from the experiment result, as shown in the inset of Fig. 3(a). Then we get a gap of 45 meV, close to the reported CDW-gap value of 50 meV by STM experiment.¹¹ Nevertheless, the approach here should be considered as a qualitative analysis rather than a quantitative estimation, because the Drude model, which contains a frequency-independent scattering rate, is not expected to well describe the low- ω charge dynamics. In the Na_xTaS_2 case, a similar gaplike feature is obscure and shifts to lower energies for Na_xTaS_2 $T_c=2$ K sample, and almost disappears in the higher Na content crystal. Since the midinfrared peak in $\sigma_1(\omega)$ appears only below T_{CDW} for the CDW-bearing samples, and vanishes for the sample without CDW, which agree with the dc transport results, therefore this peak in $\sigma_1(\omega)$ has a CDW origin. As the Drude contribution coexists with the midinfrared peak below T_{CDW} , the Fermi surface is only partially gapped in the CDW state.

It is well known that a partial gap structure can be well resolved in the frequency-dependent scattering rate $\Gamma(\omega)$.^{10,12}

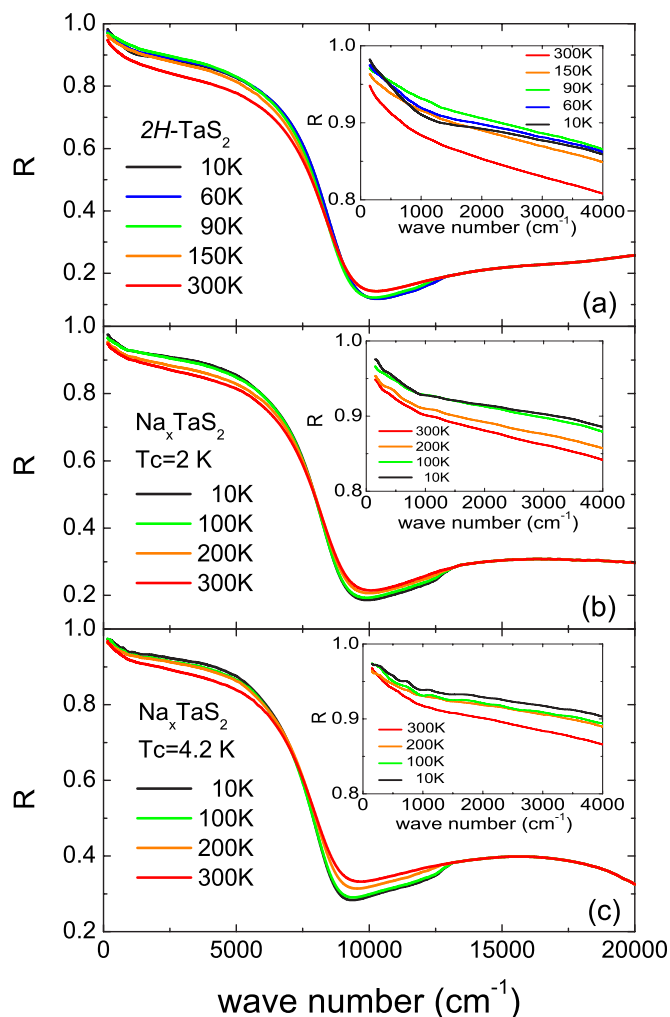


FIG. 2. (Color online) Reflectivity of (a) $2H$ - TaS_2 , (b) Na_xTaS_2 ($T_c=2$ K), and (c) Na_xTaS_2 ($T_c=4.2$ K) from 150 to 20 000 cm^{-1} at various temperatures. The inset figures focus on the spectra from 150 to 4000 cm^{-1} .

Figure 4 shows the $\Gamma(\omega)$ spectra obtained from the extended Drude model $\Gamma(\omega)=(\omega_p^2/4\pi)\text{Re}[1/(\sigma(\omega))]$, where ω_p is the overall plasma frequency and can be obtained by summarizing $\sigma_1(\omega)$ up to the reflectance edge frequency. The obtained ω_p values are roughly 2.4×10^4 cm^{-1} for $2H$ - TaS_2 , 2.6×10^4 cm^{-1} for Na_xTaS_2 $T_c=2$ K sample, and 3.0×10^4 cm^{-1} for Na_xTaS_2 $T_c=4.2$ K sample. For $2H$ - TaS_2 , above T_{CDW} , $\Gamma(\omega)$ is almost unchanged in shape but decreases in magnitude as T decreases; while in the CDW state, a broad peak forms around 1000 cm^{-1} and gets stronger at 10 K. For Na_xTaS_2 , a similar feature becomes weaker and shifts slightly to lower energies for $T_c=2$ K sample and tends to vanish for the sample with a higher Na content. We note that the spectral feature in $\Gamma(\omega)$ is very similar to that of other materials which have a partially gapped Fermi surface, such as the antiferromagnet Cr where a spin-density-wave gap opens on parts of the FS,¹² and the electron-doped high- T_c cuprate $\text{Nd}_{2-x}\text{Ce}_x\text{CuO}_4$ in which a spin-correlation gap appears at “hot spots” (the intersecting points of the FS with the antiferromagnetic zone boundary).¹⁰ In comparison with

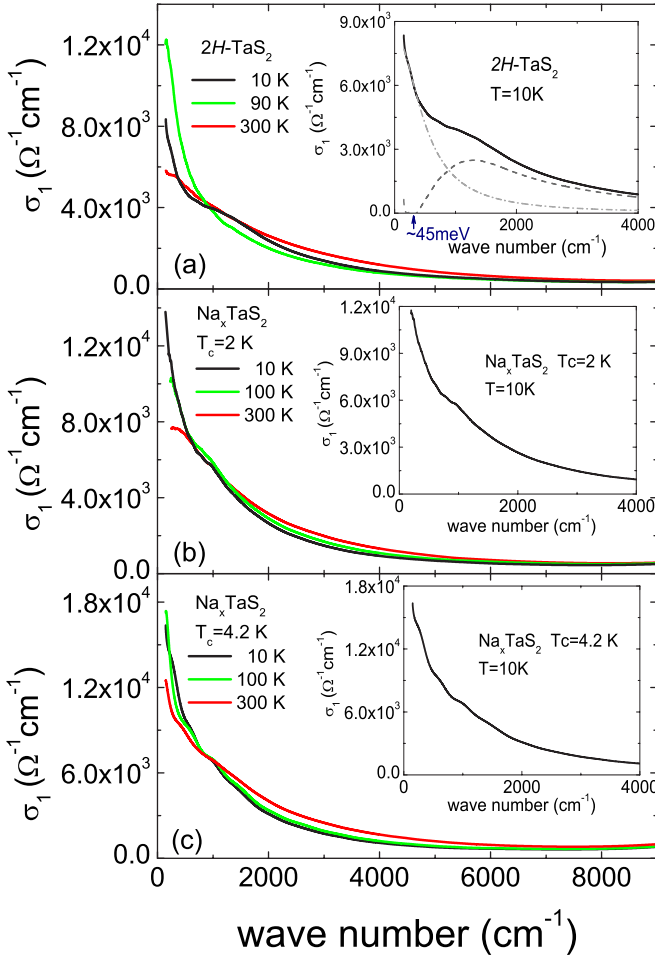


FIG. 3. (Color online) The real part of conductivity of (a) $2H\text{-TaS}_2$, (b) Na_xTaS_2 ($T_c=2$ K), and (c) Na_xTaS_2 ($T_c=4.2$ K) from 150 to 9000 cm^{-1} at selected temperatures. The insets amplify the spectra at 10 K from 150 to 4000 cm^{-1} . For $2H\text{-TaS}_2$, the experiment data, a Drude fit, and the result of $\sigma_1(\omega)$ minus Drude fit are plotted by a black line, a gray dash dot line, and a dark gray dash line, respectively.

those works, the $\Gamma(\omega)$ spectra shown in Fig. 4 further clarify the existence of CDW partial gap on the FS in $2H\text{-TaS}_2$ and its vanishing tendency upon Na intercalation. We emphasize that the CDW-gap feature in optics is weak in $2H\text{-TaS}_2$. Early work based on other technique indicated that only 10%–20% FS were removed by the CDW gap in $2H\text{-Ta}$ materials.³ Qualitatively, our result is consistent with those work.

III. DISCUSSION

A. Scattering rate in the normal phase

In the above section, we have identified the weak peak structure in the scattering rate spectrum $\Gamma(\omega)$ as due to the formation of a partial energy gap in the CDW phase. On the other hand, the $\Gamma(\omega)$ of $2H\text{-TaS}_2$ in the normal phase ($T > T_{CDW}$) exhibits a linear frequency dependence over a broad energy range [see Fig. 4(a)]. Such linear dependence

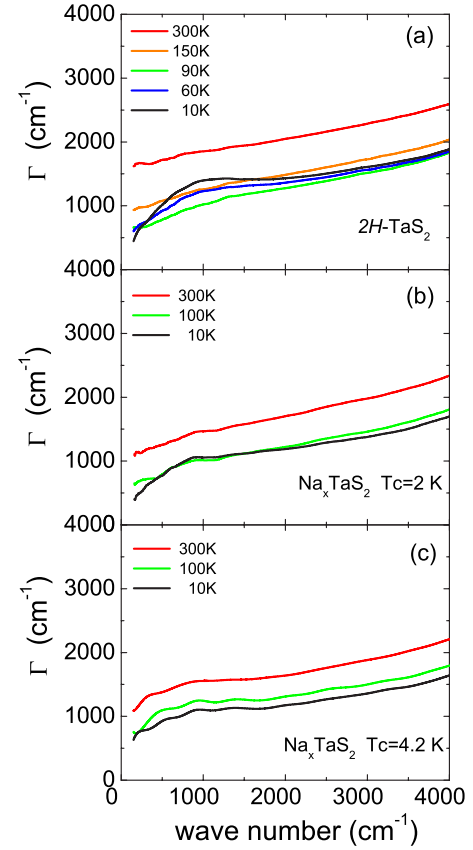


FIG. 4. (Color online) The scattering rate of (a) $2H\text{-TaS}_2$, (b) Na_xTaS_2 ($T_c=2$ K), and (c) Na_xTaS_2 ($T_c=4.2$ K).

in scattering rate appears to be a common feature for $2H\text{-TMDC}$ family because a similar behavior was found for two other members $2H\text{-NbSe}_2$ and $2H\text{-TaSe}_2$ with $\omega > 500$ cm^{-1} .^{7,8} The deviation from the ω^2 dependence of $\Gamma(\omega)$ suggests that the metallic phase is not a standard Fermi liquid. As the ω^2 dependence is observed in some three-dimensional (3D) metals or compounds which tend to become coherent 3D-like, for example, in antiferromagnet Cr (Ref. 12) and heavily overdoped high- T_c cuprates,¹⁰ such linear- ω dependence of $\Gamma(\omega)$ may be ascribed to its quasi-two-dimensional (quasi-2D) character of $2H\text{-TMDC}$. Note that the normal state scattering rates of two Na_xTaS_2 samples in Figs. 4(b) and 4(c) deviate slightly from the linear- ω dependence, especially for the higher Na content crystal. In fact, a slight increase of sodium content in Na_xTaS_2 can reduce the anisotropy of resistivity ρ_c/ρ_{ab} , thus weakening the quasi-2D character of $2H\text{-TaS}_2$.² Additionally, the disorder effect induced by the sodium may also contribute to the deviation.

B. CDW gap in $2H\text{-TMDC}$

As shown in Sec. II, we identified the formation of a CDW induced partial gap in $2H\text{-TaS}_2$ and the spectral evolution after Na intercalation. In comparison with other CDW-bearing $2H\text{-TMDC}$ members, i.e., $2H\text{-NbSe}_2$, and $2H\text{-TaSe}_2$, the spectral change across the CDW transition is significantly

different. For $2H\text{-NbSe}_2$ ($T_{CDW}=33$ K), no apparent changes were found in $\sigma_1(\omega)$ from the normal state to the CDW phase, except that the Drude peak turns sharper with decreasing temperature.⁷ For $2H\text{-TaSe}_2$ ($T_{CDW}=122$ and 90 K), a pseudo-gap-like feature exists even at room temperature and gradually moves to higher energies when the temperature goes down, thus no sudden feature develops in coincidence with the onset of the CDW.⁸ In our study of $2H\text{-TaS}_2$, the gap feature emerges only below T_{CDW} , as illustrated in Fig. 4(a). Since the gap character in $2H\text{-TaS}_2$ is more evident and its emergence clearly corresponds with the CDW transition, it is therefore an ideal system to study the charge-density-wave nature in $2H\text{-TMDC}$ family.

C. CDW mechanism

Before giving further discussion on the charge-density-wave mechanism, a brief review about angle-resolved photoelectron spectroscopy (ARPES) on $2H\text{-TMDC}$ is necessary. Previous studies on $2H\text{-NbSe}_2$,^{13–16} $2H\text{-TaS}_2$ ¹⁵ and $2H\text{-TaSe}_2$ (Refs. 17 and 18) showed that they all have similar Fermi surfaces, i.e., two double-wall hole pockets around Γ and K . In particular, recent research indicates that Na_xTaS_2 also has such two-pocket Fermi surface.⁶ Apart from observations of the FS topology, the existence of a saddle point at $1/2$ ΓK ,¹⁴ or an extended saddle band along ΓK ,^{15,17,19} was also confirmed by ARPES for $2H\text{-TMDC}$ members.

The key requirement for any CDW mechanism is a direct observation of the CDW gap and a match between the nesting vector which links the gapped region and the CDW vector associated with the lattice superstructure. Fermi surface nesting is a traditional mechanism for the CDW transition, which predicts the opening of charge-density-wave gap at parallel regions of the Fermi surface connected by the CDW vector. For $2H\text{-TMDC}$ members, the possibility of the Γ pocket self-nesting at parallel hexagon boundaries¹⁴ has been excluded because the distance between two nesting parts does not match the length of the CDW vector associated with the nearly 3×3 superlattice, and no CDW gap was found around the Γ pocket.^{6,15–20} On the other hand, there are evidences for a weak nesting at the Fermi surface around K ,^{3,16,18,21} and the energy gap around the inner K pocket below T_{CDW} was clearly observed in $2H\text{-TaSe}_2$ (Refs. 17 and 18) and $2H\text{-TaS}_2$.¹⁵ Besides the FS nesting scenario, the saddle point mechanism is another traditional model which regards the saddle points close to E_F as scattering “sink,” and their removal in the CDW state will enhance the dc conductivity.⁴ However, the saddle point’s position as observed by ARPES would lead to a 2×2 superlattice, inconsistent with the nearly 3×3 superlattice for $2H\text{-TMDC}$ in the CDW state. Moreover, the saddle band is not so close to the Fermi energy^{14–16} as Rice and Scott predicted. Therefore, some recent ARPES studies try to find other “hidden” orders in the k space to explain the CDW instability, such as the CDW-vector-matched saddle points where the “gap” follows BCS description⁵ or special “gapped” regions around the M point of the Brillouin zone.⁶ In fact, M is close to the K pocket, and the appearance of a gap around M is usually accompanied by the opening of a real CDW gap on the FS

around the K pocket. In particular, for energy band which does not cross E_F , the observation of spectral change is not a real gap but an “energy shift,”^{17,19} so the gapped region around M cannot account for charge-density-wave instability in $2H\text{-TMDC}$.

Optical probe offers supplementary information on charge excitations with high energy resolution, and its result should be consistent with ARPES observation. On this basis, our data can be naturally understood in the frame of Fermi surface nesting mechanism. First of all, we observe the temperature evolution of a partial gap formed on the Fermi surface, which is directly related to the onset of charge-density-wave transition. For $2H\text{-TaS}_2$, both the suppression in $R(\omega)$, the midinfrared peak in $\sigma_1(\omega)$, and the broad peak in $\Gamma(\omega)$ below T_{CDW} testify the existence of a gapped Fermi surface in the CDW state. All those characters turn weaker after Na intercalation, and tend to disappear with increasing Na content, which again convinces us that they have a CDW origin. As the Drude component in $\sigma_1(\omega)$ never disappears at all temperatures, the free-carrier contribution exists in the CDW state, in agreement with the fact that the Γ pocket is unaffected in the CDW state for both $2H\text{-TaS}_2$ (Ref. 15) and the low Na content Na_xTaS_2 .⁶ ARPES experiments indicate that the Γ pocket dominates the transport properties,²⁰ while formation of a CDW gap at the K pocket, which plays a lesser role in transport above T_{CDW} , would reduce the scattering channels, therefore enhancing the metallic behavior in the CDW state, so that the resistivity drops quickly below T_{CDW} for $2H\text{-TaS}_2$ and Na_xTaS_2 $T_c=2$ K samples. The FS nesting mechanism can also help in understanding why Na intercalation suppresses the CDW transition and increases T_c . As evidenced by ARPES experiments, both the inner and outer K pockets contribute to superconductivity by opening up superconducting gaps below T_c in regions which are not gapped by CDW ordering.^{22,23} Here, we should keep in mind that only certain regions of the inner K pocket satisfy the CDW nesting condition.^{3,16,18,21} With Na intercalation, the Fermi surfaces surrounding both Γ and K are expected to change. This was confirmed by recent ARPES research on Na_xTaS_2 crystals.⁶ Then it is possible that some parts of the Fermi surface around the K pocket would no longer be nested upon Na intercalations, leading to a gradual reduction of the gapped regions; therefore the CDW-gap feature in $\sigma_1(\omega)$ and $\Gamma(\omega)$ for Na_xTaS_2 crystals are weaker than that of $2H\text{-TaS}_2$. As fewer FS around the K pocket can be gapped in the CDW state, density of states at Fermi energy would be larger than the case in $2H\text{-TaS}_2$. Following BCS theory, T_c will increase as a result.

IV. CONCLUSION

We studied the optical properties of $2H\text{-TaS}_2$ and Na_xTaS_2 over a broad frequency range at various temperatures. Both the midinfrared suppression in $R(\omega)$, the peak in $\sigma_1(\omega)$, and $\Gamma(\omega)$ appear in accord with the onset of CDW transition, thus signaling the formation of a partial gap on the Fermi surface in the CDW state. The gradual removal of CDW characters for two different Na_xTaS_2 samples further confirms that the gaplike features observed in $2H\text{-TaS}_2$ have

a CDW origin. The charge-density-wave mechanism in 2H-TMDC and Na's role in the suppression of CDW can be understood in the frame of Fermi surface nesting mechanism. Specifically, we suggest that the K pocket is not only responsible for the CDW instability, but also contributes largely to superconductivity.

ACKNOWLEDGMENTS

This work is supported by the National Science Foundation of China, the Knowledge Innovation Project of the Chinese Academy of Sciences, and the 973 project of the Ministry of Science and Technology of China.

*nlwang@aphy.iphy.ac.cn

- ¹J. A. Wilson and A. D. Yoffe, *Adv. Phys.* **18**, 193 (1969); J. A. Wilson, F. J. Di Salvo, and S. Mahajan, *ibid.* **24**, 117 (1975); D. E. Moncton, J. D. Axe, and F. J. DiSalvo, *Phys. Rev. B* **16**, 801 (1977).
- ²L. Fang, Y. Wang, P. Y. Zou, L. Tang, Z. Xu, H. Chen, C. Dong, L. Shan, and H. H. Wen, *Phys. Rev. B* **72**, 014534 (2005).
- ³J. A. Wilson, *Phys. Rev. B* **15**, 5748 (1977).
- ⁴T. M. Rice and G. K. Scott, *Phys. Rev. Lett.* **35**, 120 (1975).
- ⁵O. Seifarth, S. Gliemann, M. Skibowski, and L. Kipp, *J. Electron Spectrosc. Relat. Phenom.* **137-140**, 675 (2004).
- ⁶D. W. Shen *et al.*, arXiv:cond-mat/0612064 (unpublished).
- ⁷S. V. Dordevic, D. N. Basov, R. C. Dynes, and E. Bucher, *Phys. Rev. B* **64**, 161103(R) (2001).
- ⁸A. S. Barker, Jr., J. A. Ditzenberger, and F. J. Di Salvo, *Phys. Rev. B* **12**, 2049 (1975); V. Vescoli, L. Degiorgi, H. Berger, and L. Forro, *Phys. Rev. Lett.* **81**, 453 (1998); S. V. Dordevic *et al.*, *Eur. Phys. J. B* **33**, 15 (2003).
- ⁹A. R. Beal, H. P. Hughes, and W. Y. Liang, *J. Phys. C* **8**, 4236 (1975); S. S. P. Pakkin and A. R. Beal, *Philos. Mag. B* **42**, 627 (1980).
- ¹⁰N. L. Wang, G. Li, Dong Wu, X. H. Chen, C. H. Wang, and H. Ding, *Phys. Rev. B* **73**, 184502 (2006).
- ¹¹C. Wang, B. Giambattista, C. G. Slough, R. V. Coleman, and M. A. Subramanian, *Phys. Rev. B* **42**, 8890 (1990).
- ¹²D. N. Basov, E. J. Singley, and S. V. Dordevic, *Phys. Rev. B* **65**, 054516 (2002).
- ¹³T. Kiss, T. Yokoya, A. Chainani, S. Shin, M. Nohara, and H. Takagi, *Physica B* **312-313**, 666 (2002).
- ¹⁴T. Straub, T. Finteis, R. Claessen, P. Steiner, S. Hufner, P. Blaha, C. S. Oglesby, and E. Bucher, *Phys. Rev. Lett.* **82**, 4504 (1999).
- ¹⁵W. C. Tonjes, V. A. Greanya, R. Liu, C. G. Olson, and P. Molinie, *Phys. Rev. B* **63**, 235101 (2001).
- ¹⁶K. Rossmagel, O. Seifarth, L. Kipp, M. Skibowski, D. Voß, P. Kruger, A. Mazur, and J. Pollmann, *Phys. Rev. B* **64**, 235119 (2001).
- ¹⁷R. Liu, W. C. Tonjes, V. A. Greanya, C. G. Olson, and R. F. Frindt, *Phys. Rev. B* **61**, 5212 (2000).
- ¹⁸K. Rossmagel, Eli Rotenberg, H. Koh, N. V. Smith, and L. Kipp, *Phys. Rev. B* **72**, 121103(R) (2005).
- ¹⁹R. Liu, C. G. Olson, W. C. Tonjes, and R. F. Frindt, *Phys. Rev. Lett.* **80**, 5762 (1998).
- ²⁰T. Valla, A. V. Fedorov, P. D. Johnson, J. Xue, K. E. Smith, and F. J. DiSalvo, *Phys. Rev. Lett.* **85**, 4759 (2000).
- ²¹G. Wexler and A. M. Woolley, *J. Phys. C* **9**, 1185 (1976).
- ²²T. Valla, A. V. Fedorov, P. D. Johnson, P.-A. Glans, C. McGuinness, K. E. Smith, E. Y. Andrei, and H. Berger, *Phys. Rev. Lett.* **92**, 086401 (2004).
- ²³T. Yokoya, T. Kiss, A. Chainani, S. Shin, M. Nohara, and H. Takagi, *Science* **294**, 2518 (2001).